A semi-synthetic red light photoswitch for optogenetic control of protein activity

Yuto Kuwasaki
The University of Tokyo
Kazushi Suzuki
The University of Tokyo
Gaigai Yu
The University of Tokyo
Yuki Kakihara
The University of Tokyo
Michiru Nishiwaki
The University of Tokyo
Keiji Fushimi
Shizuoka University
Ramsey Bekdash
Columbia University
Yoshihiro Shimizu
RIKEN https://orcid.org/0000-0003-3499-1394
Rei Narikawa
Shizuoka University
Takahiro Nakajima
The University of Tokyo
Masayuki Yazawa
Columbia University https://orcid.org/0000-0002-5730-6583
Moritoshi Sato (moritoshisato@g.ecc.u-tokyo.ac.jp)
University of Tokyo https://orcid.org/0000-0002-3095-5831

Article

Keywords: Mammalian Deep Tissues, Bacterial Phytochrome, Endogenous Chromophore, Biliverdin, de novo Synthetic Binder, Split Protein Reassembly, CRISPR-Cas9 System

Posted Date: May 5th, 2021

DOI: https://doi.org/10.21203/rs.3.rs-450425/v1

Version of Record: A version of this preprint was published at Nature Biotechnology on June 13th, 2022.
See the published version at https://doi.org/10.1038/s41587-022-01351-w.

A semi-synthetic red light photoswitch for optogenetic control of protein activity

Yuto Kuwasaki[1], Kazushi Suzuki[1], Gaigai Yu[1], Yuki Kakihara[1], Michiru Nishiwaki[1], Keiji Fushimi[2], Ramsey Bekdash[3,4], Yoshihiro Shimizu[5], Rei Narikawa[2], Takahiro Nakajima[1,6], Masayuki Yazawa[4,5] and Moritoshi Sato[1*]

[1] Graduate School of Arts and Sciences, The University of Tokyo, Komaba, Meguro-ku, Tokyo, Japan.

[2] Graduate School of Integrated Science and Technology, Shizuoka University, Shizuoka, Japan.

[3] Department of Rehabilitation and Regenerative Medicine, Columbia Stem Cell Initiative, Columbia University, New York, USA

[4] Department of Molecular Pharmacology and Therapeutics, Columbia University, New York, USA

[5] Laboratory for Cell-Free Protein Synthesis, Quantitative Biology Center, RIKEN, Suita, Osaka, Japan.

[6] Kanagawa Institute of Industrial Science and Technology, Kanagawa, Japan.

Corresponding author

*Email: moritoshisato@g.ecc.u-tokyo.ac.jp

Abstract: 150 words (147 words)

Red light is useful for optogenetic control of various protein activities in mammalian deep tissues due to its high tissue penetration, low invasiveness, and low light scattering. However, technology that enables for the optogenetic manipulation using red light remains elusive. Here we develop a red light-activatable, semi-synthetic photoswitch, named MagRed. MagRed is composed of a red light-absorbing bacterial phytochrome incorporating a mammalian endogenous chromophore, biliverdin, and its photo-state-specific *de novo* synthetic binder. MagRed allows us to reassemble split-proteins using red light and thereby develop a red light-activatable Cre recombinase, which is applicable for mammalian deep tissues. Additionally, we take advantage of MagRed to develop red light-inducible transcription system based on the CRISPR-Cas9 system, enabling for high induction (up to 378-fold) of multiple user-defined endogenous target genes. With high versatility and regulatability, MagRed provides a powerful technology that easily facilitates optogenetics applications for a variety of biological research areas.

Introduction: 3,000 words (3630 words)

Blue light-activatable photoswitches, such as CRY2-CIB1[1], iLID-sspB[2] and the Magnet system[3], have emerged as a powerful core technology to directly manipulate protein activity using blue light with high spatiotemporal resolution in mammalian cells[4,5]. For example, by recruiting functional domains to the plasma membrane or the promoter region of a gene of interest using the photoswitches, cellular functions such as cellular dynamics[2], signal transduction[6] and gene expression[7,8], can be manipulated by blue light. Beyond the domain-recruitment strategy, a more robust strategy based on reassembling split-protein fragments using the blue light-activatable photoswitches have been developed and widely applied in various protein classes including nucleases[9,10], recombinases[11,12], proteases[13], polymerases[14], antibodies[15] and neurotoxins[16]. Using blue light-activatable photoswitches to reassemble split-proteins has greatly expanded the range of optogenetically controllable molecular processes in the cell, allowing researchers to address otherwise intractable biological questions. However, blue light is easily scattered and absorbed in mammalian tissues, greatly impairing the applicability of blue light-activatable photoswitches in deep tissues[17].

In contrast to blue light illumination, red light illumination through the tissue transparency window (650~900 nm) is highly advantageous for the optogenetic manipulation in mammalian deep tissues due to its high tissue transparency, low invasiveness and low light scattering. Several red light-activatable photoswitches have been developed using red light-absorbing phytochromes from plants and cyanobacteria, and tested for optogenetic manipulation in living cells[18–20]. However, the plant/cyanobacterial phytochrome-based photoswitches require exogenous chromophores such as phytochromobilin and phycocyanobilin to absorb red light and function[21], which limits their use in mammalian systems. Bacterial phytochromes can function by incorporating an endogenous chromophore biliverdin (BV) in mammalian cells. One of the bacterial phytochromes, BphS, is activated by red light to convert guanylate triphosphate (GTP) into cyclic diguanylate monophosphate (c-di-GMP). BphS allows for red-light inducible transcription of a target gene by using it together with additional modules, such as the c-di-GMP-responsive hybrid transactivator p65-VP64-NLS-BldD, the chimeric promoter P_{FRLx} and YhjH phosphodiesterase[22,23]. However, the BphS-based system requiring many components is complicated, does not enable for direct manipulation of protein activity, and could cause adverse effects on mammalian cells through an endogenous target of c-di-GMP. Recently, a red light photoswitch based on a bacterial phytochrome from *Rhodopseudomonas palustris* (RpBphP1) and its binding partner has been developed[24,25]. RpBphP1 shows reversible photoconversion between a Pfr dark-state and a Pr

78 photo-state. Upon red light illumination, RpBphP1 is converted to the Pr photo-state and forms
79 a heterodimer with its binding partner PpsR2 or its downsized variant QPAS1, thereby being
80 applicable to simply and directly manipulating protein activity.
81 In this study, we demonstrate that RpBphP1-PpsR2/QPAS1 has two serious
82 weaknesses: First, RpBphP1-PpsR2/QPAS1 does not work well for the split-protein
83 reassembly strategy while being applicable to the domain-recruitment strategy, thereby limiting
84 its use for optogenetic applications. Second, PpsR2 binds not only to the holo-protein of
85 RpBphP1 upon red light illumination but also to its apo-protein irrespective of red light
86 illumination. The light-independent binding of PpsR2 with the apo-protein of RpBphP1 causes
87 spontaneous activation of the optogenetic tools in the dark condition and thereby greatly
88 hampers their regulatability. These benchmarking studies reveal that core technology with high
89 versatility and regulatability that enables for the optogenetic manipulation using red light
90 remains elusive.
91 To better facilitate optogenetics using red light, we developed a red light-activatable,
92 semi-synthetic photoswitch, named MagRed. MagRed is composed of a red light-absorbing,
93 BV-binding bacterial phytochrome derived from *Deinococcus radiodurans* (DrBphP) and its
94 photo-state-specific *de novo* synthetic binder. Compared to RpBphP1-PpsR2/QPAS1, MagRed
95 has higher versatility that enables for split-protein reassembly strategy with red light
96 illumination. Based on MagRed and split-Cre fragments, we developed a red light-activatable
97 Cre recombinase, enabling for DNA recombination upon red light illumination in mammalian
98 deep tissues. Additionally, we applied MagRed to the domain-recruitment strategy to develop
99 a red light-activatable, highly efficient optogenetic gene expression system based on the
100 CRISPR-Cas9 system, enabling high induction (up to 378-fold) of multiple user-defined
101 endogenous gene targets. The MagRed-based optogenetic tools have robust and precise
102 regulatability and do not exhibit leak activation in the dark regardless of BV concentration in
103 the cell, thereby overcoming the limitation of RpBphP1-PpsR2, which has been troubled by
104 the leak activation in the dark. We also show that MagRed has reliable regulatability in terms
105 of mutually independent ON/OFF switching using two-colored light illuminations and
106 sustainable ON-switching even with pulsed illumination.

Result

Development of MagRed.

To develop a red light photoswitch, we applied synthetic biological approaches to generate a photo-state specific *de novo* binding partner of DrBphP, a bacterial phytochrome derived from *Deinococcus radiodurans* (**Fig. 1a**). DrBphP incorporates BV as a mammalian endogenous chromophore and reversibly photoconverts between a Pr dark-state (λ_{max} = 701 nm) and a Pfr photo-state (λ_{max} = 752 nm) with two-wavelength light illuminations (**Supplementary Fig. 1a**). In addition to the chromophore availability in mammalian cells and the controllability using two-colored light illuminations, previous studies have revealed that the photosensory core module of DrBphP, hereafter referred to as DrBphP-PSM, undergoes a light-induced large conformational change between the Pr dark-state and the Pfr photo-state[26] (**Supplementary Fig. 1b**). The large conformational change of DrBphP is an advantage for developing its *de novo* synthetic binder that selectively binds to the Pfr photo-state but not to the Pr dark-state. Importantly, previous studies reported that DrBphP exhibits biexponential slow dark reversion kinetics with decay amplitude of 24% for 7 min and with that of 76% for the following 1,291 min[27,28], which is much slower than that of RpBphP1 ($t_{1/2}$=2.83 min[24]) (**Supplementary Fig. 2**). The slow dark reversion kinetics of DrBphP is beneficial for keeping it associated with the photo-state specific binder even after turning off red light illumination, thereby enabling for a sustained activation of optogenetic tools even by single or pulsed illumination. In contrast, RpBphP1 does not have such a controllability due to its fast dark reversion kinetics[24].

To generate a binding partner of DrBphP, we applied Affibody, the Z domain of immunoglobulin-binding *staphylococcal* protein A. Thirteen residues in the first and second helices of Affibody were randomized to generate its ribosome-displayed library[29] (**Fig. 1b**). We purified the DrBphP-PSM protein and immobilized it on magnetic beads, and then performed *in vitro* selections using the Affibody library to obtain binders for DrBphP-PSM under the 660 nm and the 760 nm light illumination conditions, respectively. After six rounds of the selections, we sequenced the cDNA library and eliminated Affibody clones detected under both the 660 nm and the 760 nm light illumination conditions. Finally, we prioritized Affibody clones with high read counts detected only under the 660 nm condition (**Supplementary Table 1**).

We assessed whether the top 10 candidates of the prioritized Affibody clones could interact with DrBphP-PSM in mammalian cells by the tetR-tetO-based firefly luciferase (fluc) expression system with VP16, a transcription activation domain (**Fig. 1c**). Of the tested clones, one Affibody clone named Aff6 displayed a high bioluminescence intensity upon red light

illumination at 660 nm, which was comparable with that induced by a direct fusion of tetR and VP16 (**Fig. 1d, e, Supplementary Fig. 3**). This result indicates that Aff6 binds to the Pfr photo-state of DrBphP-PSM with a high affinity. However, its Light/Dark contrast was considerably low (1.2 fold-induction) because it also showed a substantially high leakiness in the dark. We found that the leak in the dark was significantly decreased by using the full-length DrBphP instead of DrBphP-PSM (**Fig. 1e**). However, the full-length DrBphP, hereafter referred to as just DrBphP, also decreased the bioluminescence intensity upon red light illumination, resulting in the low Light/Dark contrast (1.6 fold-induction). We thus focused on a directed evolution of Aff6 to improve its interaction with DrBphP. At first, we introduced individual alanine substitutions into the randomizable 12 residues of Affi6. V18A substitution of Affi6 did not significantly alter the bioluminescence intensity compared to the wild-type, whereas the other substitutions remarkably decreased the bioluminescence intensity (**Supplementary Fig. 4**). We conducted saturation mutagenesis at the V18 residue in Affi6 and found that V18F, V18W and V18H mutations significantly improved the Light/Dark contrast compared to the original Aff6 (**Fig. 1d, e and Supplementary Fig. 5**). Truncation of the N-terminal unstructured three residues from Aff6_V18F further enhanced the Light/Dark contrast (8.3-fold induction with 67% activity of tetR-VP16) (**Fig. 1d, e**). We named the pair of DrBphP and Aff6_V18FΔN "MagRed".

Photoswitching property of MagRed.

To further characterize MagRed in mammalian cells, we performed a bioluminescence assay using a split-firefly luciferase (split-fluc)[30] (**Fig. 2a, b**). In HEK 293T cells expressing MagRed-fused split-fluc, repeated induction of bioluminescence was feasible using the 660 nm and the 800 nm pulsed illuminations (**Fig. 2c**). This result demonstrates that the two-colored pulsed illuminations can independently and repeatedly control the association (switch-ON) and the dissociation (switch-OFF) of MagRed. Next, we measured the dissociation kinetics of MagRed. After the 660 nm illumination was turned off, MagRed maintained its association form with approximately 70% efficiency, following 21 % decrease for the first 10 min (**Fig. 2d**). This biphasic slow dissociation kinetics of MagRed is correlated with the biexponential slow dark reversion kinetics of DrBphP (**Supplementary Fig. 6**), showing that the slow dark reversion kinetics of DrBphP is an essential factor for developing MagRed with a high controllability as expected.

Red light-activatable transcription system to control endogenous expressions.

To investigate the suitability of MagRed to domain-recruitment applications, we applied MagRed to CRISPR-Cas9-based photoactivatable transcription system (CPTS)[7,8]. In this system, MagRed plays a role in the red light-dependent recruitment of transcription activation domains, p65 and HSF1, to target loci, harboring inactive Cas9 (dCas9), sgRNA-bearing MS2 RNA aptamer and MS2 coat protein (**Fig. 3a**). We designed all configurations for CPTS and examined their transcription activities using a luciferase reporter (**Fig. 3b**). In addition, we also tested the existing red light photoswitch RpBphP1-PpsR2/QPAS1 in CPTS as benchmark experiments to compare with MagRed. Most of the configurations for CPTS using MagRed showed significantly high Light/Dark contrasts, which were up to 70-fold induction (**Fig. 3b-d, and Supplementary Fig. 7a**). On the other hand, all the configurations for CPTS using RpBphP1-PpsR2/QPAS1 showed much lower Light/Dark contrasts, which were up to 4.2-fold induction (**Fig. 3b-d**). We found that the low Light/Dark contrasts of RpBphP1-PpsR2/QPAS1-based CPTS were attributable to their high leak activities in the dark (**Supplementary Fig. 7b, c**). These results demonstrate that MagRed can control the domain recruitment more precisely and dynamically than RpBphP1-PpsR2/QPAS1 in CPTS.

To examine why RpBphP1-PpsR2/QPAS1-based CPTS shows high leak activity in the dark, we accessed the effect of BV concentration on its transcription activity. We found that the addition of excess amount of BV decreased the dark leak activity of CPTS based on RpBphP1-PpsR2/QPAS1 (P=0.00781, **Supplementary Fig. 8a, b**). Following this result, we hypothesized that the apo-protein of RpBphP1, which is not yet incorporated with BV, could cause the high leak activation of RpBphP1-PpsR2/QPAS1-based CPTS in the dark. To examine the effect of the apo-protein of RpBphP1 on the transcription activity, we generated mutants of RpBphP1, in which the cysteine residues covalently bound to BV were substituted to alanine (C20A) and serine (C20S), respectively. These mutants exhibited high transcription activities regardless of red light illumination (**Fig. 3e**). The results indicate that PpsR2 binds not only to the holo-protein of RpBphP1 upon red light illumination but also to its apo-protein irrespective of red light illumination, thereby causing the leak activation of RpBphP1-PpsR2/QPAS1-based CPTS in the dark. In contrast, MagRed-based CPTS exhibited little leak activity in the dark even without additional BV supplementation (P=0.250, **Supplementary Fig. 8c**). Additionally, analogous mutations in DrBphP (C24A and C24S) completely eliminated the red light-dependent transcription activity of MagRed-based CPTS (**Fig. 3f and Supplementary Fig. 9**). The results demonstrate that Aff6_V18FΔN does not bind to the apo-protein of DrBphP, leading to the minimum leak activation of MagRed-based optogenetic tools in the dark.

Among the tested configurations for MagRed-based CPTS (**Fig. 3c**), we focused on the configurations #1 and #3. Additionally, taking advantage of the small size of Aff6_V18FΔN (6.2 kDa), we designed tandem fusions of Aff6_V18FΔN to enhance its apparent affinity with DrBphP. The tandem dimer of Aff6_V18FΔN substantially enhanced the transcription activity of CPTS upon red light illumination without increasing the leak activity in the dark in both configurations #1 and #3 (**Fig. 4a**). Especially, the configuration #3 with the tandem dimer of Aff6_V18FΔN resulted in an enhanced Light/Dark contrast (619-fold induction). Although we also tested the configuration #3 with the tandem trimer and tetramer of Aff6_V18FΔN, the trimer and tetramer constructs did not exhibit further enhancement of the transcription activity (**Fig. 4a**). Therefore, we concluded the configuration #3 with the tandem dimer of Aff6_V18FΔN as the best version of MagRed-based CPTS called "Red-CPTS". We confirmed that Red-CPTS works robustly in various cell lines from different origins (**Supplementary Fig. 10**). To examine whether Red-CPTS can be applicable to endogenous gene targets, we next applied Red-CPTS to multiple endogenous genes, delivering a group of four gRNAs separately targeting human *ASCL1*, *HBG1*, *IL1R2*, and *MYOD1* promoters. We found that the targeted endogenous genes were simultaneously activated in HEK 293T cells by red light. Red-CPTS significantly increased all the targeted gene transcriptions with high Light/Dark contrasts, which were up to 378-fold induction (**Fig. 4b**). Importantly, in all the targeted endogenous genes, the mRNA levels of Red-CPTS-transfected cells in the dark were comparable to those of mock-transfected cells, demonstrating that Red-CPTS has no obvious leak activity in the dark and thereby enables for robust regulation of multiplexed user-defined endogenous gene activation using red light illumination.

Red light-activatable DNA recombination system based on split-Cre reassembly.

In addition to the domain recruitment strategy applied for CPTS, next we examined whether MagRed can be applied for the split-protein reassembly with red light illumination. Among the existing optogenetic tools based on the split-protein reassembly system with the blue light-activatable photoswitches, site-specific DNA recombinase is one of the most attractive targets[11,12,20,31–33]. Especially, Cre recombinase is the most widely used DNA recombinase in biology, biotechnology and biomedical studies[34–37]. We fused MagRed to split-Cre fragments to develop a red light-activatable Cre recombinase applicable in mammalian systems (**Fig. 5a**). To test all configurations, we fused either DrBphP or Aff6_V18FΔN to the newly created N- and C-terminal ends of split-Cre fragments (CreN and CreC) as well as the original N-terminal end of CreN (**Fig. 5b**). We also tested two split positions (CreN59/CreC60 and

CreN104/CreC106) for the split-Cre fragments. The DNA recombination activities were examined using a Floxed-STOP fluc reporter in HEK 293T cells (**Supplementary Fig. 11a**). Most of the configurations using MagRed and split-Cre exhibited red light-dependent DNA recombination with significant Light/Dark contrasts (**Fig. 5b-d, and Supplementary Fig. 12a**). Of the tested configurations, NLS-CreN104-Aff6_V18FΔN and NLS-DrBphP-CreC106 gave the highest Light/Dark contrast (31-fold induction). This MagRed-based red light-activatable Cre recombinase was named "RedPA-Cre". We confirmed that additional BV supplementation did not have significant effect on the DNA recombination activity of RedPA-Cre (**Supplementary Fig. 13**), revealing that RedPA-Cre works robustly at the endogenous BV concentration of living mammalian cells as Red-CPTS does.

We also tested RpBphP1-PpsR2/QPAS1 for the split-protein reassembly strategy with split-Cre and compared their DNA recombination activities with the MagRed version. Compared to MagRed, RpBphP1-PpsR2/QPAS1 displayed much lower Light/Dark contrasts in all the tested configurations fused with split-Cre despite additional BV supplementation for eliminating the apo-protein of RpBphP1 (**Fig. 5b-d and Supplementary Fig. 12b, c**). During RedPA-Cre development, a new red light-inducible dimerization system, named nanoReD system (nanoReD1 and nanoReD2), were reported[38]. We also examined whether nanoReD systems could be applied to the split-protein reassembly with split-Cre. We found that nanoReD systems also showed much lower Light/Dark contrasts in bioluminescence intensity under any configurations with split-Cre as RpBphP1-PpsR2/QPAS1 did (**Fig. 5c, d and Supplementary Fig. 12d, e**). The results reveal that MagRed enables for the split-protein reassembly with split-Cre for the development of a red light-activatable Cre recombinase, which is not achieved by the existing red light photoswitches, RpBphP1-PpsR2/QPAS1 and nanoReD systems.

We tested various illumination conditions for the activation of RedPA-Cre using a Floxed-Stop fluc reporter. We found that all the tested conditions with different durations of red light illumination evoked significant bioluminescence induced by the DNA recombination (**Supplementary Fig. 14**). Red light illumination for only 30 s could induce DNA recombination with 38% efficiency of that induced by continuous red light illumination for 24 h, indicating that RedPA-Cre can be efficiently activated by red light illumination for even short periods of illumination time. This appears to be due to the characteristic of RedPA-Cre, which maintains its DNA recombination activity even after turning off red light illumination because of the slow dissociation kinetics of MagRed. To compare the DNA recombination activity of RedPA-Cre with that of full-length Cre (iCre), we labeled the NLS-CreN104-

Aff6_V18FΔN fragment of RedPA-Cre with a fluorescent protein Venus and then assessed its red light-inducible activity using a Floxed-STOP mCherry reporter (**Supplementary Fig. 11b**). Upon red light illumination for 24h, RedPA-Cre induced mCherry fluorescence with 55% efficiency of that induced by iCre (**Fig. 5e**).

Next, we examined whether RedPA-Cre could be applied to bicistronic designs. RedPA-Cre was able to be concatenated via an internal ribosome entry site (IRES) without compromising the red light-dependent DNA recombination and the low leak activity in the dark (**Supplementary Fig. 15**). The bicistronic RedPA-Cre was further validated *in vivo* in living mice through intrahepatic gene delivery along with a Floxed-STOP fluc reporter. We found that the exposure of the mice to red light illumination at 660 nm from the ventral side induced marked bioluminescence signals by the DNA recombination reaction in their livers (P=0.011 from n=3 mice per group, **Fig. 5f, g and Supplementary Fig. 16**). As observed in cultured cells *in vitro*, RedPA-Cre did not need additional BV supplementation to function in the liver of living mice. We also observed that the mice with RedPA-Cre exhibited little DNA recombination activity when kept in the dark. The results demonstrate that RedPA-Cre can efficiently induce DNA recombination in an internal organ in living mice even using the external and noninvasive red light illumination. We confirm that RedPA-Cre exhibits precise regulatability *in vivo*.

Discussion

After demonstration of optogenetic control of neurons with microbial opsins[39], blue light-activatable photoswitches emerged as a core technology to control various protein activities and thereby facilitate biological applications in a variety of research fields beyond neuroscience. In the next generation of optogenetics, several red light-activatable photoswitches were developed as a core technology to optogenetically manipulate protein activities through the tissue transparency window. However, such a core technology with high versatility and regulatability for enabling the optogenetic manipulation using red light remains elusive as demonstrated in this study. The lack of a powerful and useful technology is a major bottleneck hindering the development of red light optogenetic tools. To establish a better red light optogenetic technology, we applied synthetic biological approaches to develop a red light photoswitch named MagRed. MagRed can directly manipulate protein activity using red light with high spatiotemporal resolution, having two major advantages among the existing red light photoswitches in terms of versatility and regulatability.

Compared to RpBphP1-PpsR2/QPAS1 and nanoReD systems, MagRed has high versatility that enables for the split-protein reassembly with red light illumination. Based on MagRed and split-Cre, we developed RedPA-Cre, a red light-activatable Cre recombinase, allowing us to induce DNA recombination upon red light illumination in mammalian deep tissues such as livers. In addition to split-Cre, we also applied MagRed to optical control of firefly luciferase based on split-fluc reassembly, demonstrating that MagRed is generally applicable to the split-protein reassembly regardless of protein functions, sizes and structures. Split proteins can be designed for every class of proteins in principle and this has gained increased interest recently as computational approaches continue to identify new split positions of a diverse array of proteins[40,41]. These computational approaches to designing split-proteins and the present MagRed technology synergistically work to expand the range of optogenetic applications in mammalian deep tissues.

In addition to the versatility, MagRed has high regulatability that does not cause any leak activation in the dark, as opposed to RpBphP1-PpsR2/QPAS1. As optogenetic tools, the leakage of protein activity in the dark is the most serious and unacceptable weakness because it causes unintentional protein function before light stimulation, which impairs the accuracy of optogenetic control and leads to misinterpretation[33]. MagRed offers tight regulatability to optogenetic tools, thereby enabling for more precise optogenetic manipulation of protein activities. In addition, MagRed also has useful regulatability that can repeatedly control its association and dissociation by the 660 nm and 800 nm pulsed illuminations, and can maintain

the association form for a long period even after turning off the red light illumination. This regulatability of MagRed, derived from preferable switching properties of DrBphP, enables mutually independent ON/OFF switching with two-colored light illuminations and sustainable ON-switching even with pulsed illumination. Taking advantage of the useful regulatability of MagRed, we can manipulate protein activity more flexibly than with other existing tools. For example, we can terminate optogenetic manipulation at any time when we intend. Additionally, we can reduce phototoxicity on biological samples using pulsed red light illuminations. These advantages can be obtained without additional chromophore supplementation. Overall, MagRed is a unique optogenetic core technology among the existing photoswitches in respect to its high versatility and regulatability.

Using MagRed, we developed RedPA-Cre and Red-CPTS for the red light optogenetics. RedPA-Cre can efficiently induce DNA recombination with red light illumination, which is the first report on the red light activatable site-specific DNA recombinase based on split-protein reassembly, which works in mammalian systems. The Cre-*loxP* system is widely used for gene insertion, deletion, inversion, or cassette exchange in various animal models. Combined with current recombinase-based biological tools such as cell-lineage tracing[42,43], genetic circuits[44,45], and gene knock-out[33] and knock-in[46] analysis, RedPA-Cre with high spatiotemporal controllability could address more complicated biological questions and pathophysiological mechanisms for various diseases. Another MagRed-based optogenetic tool, Red-CPTS, enables activating the expression of multiplexed user-defined endogenous genes using red light illumination. In addition to transcription control, the Red-CPTS platform will also be extended to optogenetic control of other CRISPR applications based on the recruitment of effectors such as epigenetic modifications[47] and base editing[48] in mammalian deep tissues.

In conclusion, MagRed has potentials to regulate various cellular functions in a much more comprehensive range of biological samples such as living cells, mammalian deep tissues and whole animals. The remarkable features of MagRed are valuable to synergistically expand the optogenetic toolbox in the long-wavelength region, thereby opening new avenues in the field of optogenetics using red light.

Online Methods

Cloning

All 105 plasmids used in this study are listed in Supplementary Table 2, and complete cDNA sequences of these plasmids except for gifted and commercially available plasmids are denoted in Supplementary Note. All constructs that express RedPA-Cre and Red-CPTS components in HEK 293T cells, HeLa, and Neuro-2a were cloned into the pcDNA3.1 or pcDNA3.1/V5-His vector (Invitrogen, California, USA). All constructs that express tetR-tetO components were cloned into the pSV40 vector, a gift from Wilfried Weber. All constructs that encode sgRNAs were cloned into the pSPgRNA vector with the U6 promoter (Addgene plasmid # 47108).

cDNAs encoding the codon-optimized *Streptococcus pyogenes* Cas9 were amplified from pX330-U6-Chimeric_BB-CBh-hSpCas9 (Addgene plasmid #42230). To eliminate the nuclease activity of Cas9, we introduced D10A and H840A mutations in the Cas9 with the Multi Site-Directed Mutagenesis Kit (MBL) according to the manufacturer's directions. cDNAs encoding the MS2 (N55K) mutant and p65–HSF1 were amplified from MS2-P65-HSF1_GFP (Addgene plasmid #61423). The EGFP-Cre gene was amplified from pENN.AAV.hSyn.HI.eGFP-Cre.WPRE.SV40 (Addgene plasmid #105540). cDNA encoding the improved Cre recombinase (iCre) was synthesized by Invitrogen. The humanized genes encoding DrBphP, RpBphP1, and PpsR2 were synthesized by GenScript. The humanized gene encoding Zdk1 and LDB-14 (nanoReD2) was synthesized by Eurofins Genomics. The humanized gene encoding LDB-3 (nanoReD1) was synthesized by Integrated DNA Technologies. cDNAs encoding the VP16-NLS and tetR were amplified from tetR-VP16-NLS/pSV40, a gift from Wilfried Weber. The SEAP reporter plasmid pKM006 for tetR-tetO system[49] was gifted from Wilfried Weber. pKT270[50] for BV production in *E. coli* was gifted from Takayuki Kohchi.

For cloning, PCR fragments were amplified using PrimeSTAR DNA Polymerase (Takara Bio, Ohtsu, Japan). The vectors were double-digested and ligated to gel-purified PCR products by Ligation high Ver.2 (Toyobo, Osaka, Japan) or In-Fusion HD Cloning Kit (Takara Bio). Ligated plasmid products were introduced by heat shock transformation into competent Mach1 (Invitrogen) bacteria.

Absorption spectra measurements of DrBphP and RpBphP1

DrBphP and RpBphP1 proteins were expressed in *E. coli* C41 containing the bilin biosynthetic plasmid pKT270[50] in one liter LB media. After the protein expression, cells were harvested in lysis buffer (20 mM Hepes-NaOH, pH 7.5, 0.1 M NaCl and 10% (w/v) glycerol using an

Emulsiflex C5 high-pressure homogenizer at 12,000 psi (Avestin Inc., Ottawa, Canada). Homogenates were centrifuged at 165,000g for 30 min, and supernatants were filtered through a 0.8-μm cellulose acetate membrane. Filtrated samples were loaded onto a nickel-affinity His-trap column (GE Healthcare, Little Chalfont, UK) using an ÄKTAprime plus (GE Healthcare) System. The column was washed using the lysis buffer containing 50 mM and 100 mM imidazole, followed by elution using a linear gradient of the lysis buffer containing 100 to 400 mM imidazole (1 mL/min, total 15 min). After incubation with 1 mM EDTA for 1 h on ice, the purified proteins were dialyzed against the lysis buffer to remove EDTA and imidazole. Purified proteins concentration was determined by the Bradford method.

UV-Vis absorption spectra of the DrBphP and RpBphP1 proteins were recorded with a UV-2600 spectrophotometer (Shimadzu, Kyoto, Japan) at 37 °C, using a thermostated cuvette holder. An Opto-Spectrum Generator (Hamamatsu Photonics, Inc., Shizuoka, Japan) was used for generating 700 nm or 660 nm light for the photoconversion from the Pr dark-state to Pfr photo-state of DrBphP and 760 nm for the photoconversion from the Pfr dark-state to Pr phot-state of RpBphP1.

Affibody ribosome display library construction

Oligonucleotides used for "Affibody ribosome display library construction" were listed in Supplementary Table 3. The synthetic gene encoding the Affibody library was constructed by three-step PCR reactions of the Affibody library, followed by ligation with the required sequence elements for ribosome display. The dsDNA encoding the first and second helices of the Affibody was assembled by annealing and enzymatically extending primers O1 and O2 with complementary 3′ ends. Codon NNK (N = G, A, C, T; K = G, T) was used to encode randomized residues. Next, the third helix was appended by overlap extension PCR using primers O3 and O4, and the first reaction product as a template. In the third PCR, the resultant dsDNA encoding the Affibody library was amplified by PCR using primers O5 and O6 with the T7 promoter. In parallel, a genetic element including SecM elongation arrest sequence (AKFSTPVWISQAQGIRAGPQRLT) was amplified by PCR using primers O7 and O8, and pDgIIISecM-PURF1 as a template. These two fragments were digested with Type IIS restriction enzyme BsmBI (NEB, Massachusetts, USA), followed by ligation of each fragment using Ligation high Ver.2. To avoid overamplification and error in PCR, we used KOD -Multi&Epi- DNA polymerase (Toyobo), and set the cycle number of each PCR step no more than 5 cycles. Each product and ligation product were separated by gel electrophoresis and

purified with PureLink PCR Purification Kit (Invitrogen) after that subsequent reactions were carried out.

Ribosome display

A sequence encoding DrBphP-PSM was cloned into the pColdI vector (Takara Bio) containing N-terminal His6 tag followed by an Avi tag. *E. coli* C41(DE3) strain (Lucigen, Wisconsin, USA) harboring pKT270 was transformed with pColdI-Avi-DrBphP-PSM. The transformed cells were grown at 37 ºC with shaking at 200 rpm to an OD_{590}=0.45 in 30 ml LB media supplemented with ampicillin (100 mg/ml) and chloramphenicol (30 mg/ml), and the culture was cooled to room temperature. Then, isopropyl-β-D-thiogalactoside (IPTG, Wako Pure Chemistry Industries, Ltd., Osaka, Japan) and biliverdin (BV, Frontier Scientific Inc., Utah, USA) were added to the culture in a final concentration of 0.5 mM and 100 μM. The cells were cultured for 48 hours at 16 ºC in the dark for protein expression. The cultured cells were collected by centrifugation and lysed with 2 ml B-PER reagent (Thermo Fisher Scientific, Massachusetts, USA) containing 0.2 mg lysozyme (Wako Pure Chemical Industries), 10 Units DNase I (Thermo Fisher Scientific) and protease inhibitor cocktail (Sigma-Aldrich, Missouri, USA) for 10 minutes at room temperature. The crude soluble extract was purified using a HisTrap FF column (GE Healthcare). Biotinylation of DrBphP-PSM was performed using a BirA enzyme (BirA500, Avidity LLC, Colorado, USA) following the manufacturer's protocol. The ribosome-protein fusion libraries were generated with the PURE system. The standard PURE translation mixture was prepared as described previously[51]. *In vitro* transcription and translation reaction were performed at 37 ºC for 60 minutes, followed by stopping the reaction with 100 μl of TBS-Mg^{2+} buffer (50 mM Tris-HCl, 50 mM $MgCl_2$ and 150 mM NaCl, pH 7.5). Meanwhile, 30 μl volumes of streptavidin magnetic beads (Dynabeads M-280 Streptavidin, Invitrogen) were washed once with 200 μl TBS-Mg^{2+} buffer. Biotinylated DrBphP-PSM protein were added to the washed beads and incubated at 4 °C for 30 minutes with gentle rotation. The beads were then washed once with 200 ml of TBS-Mg^{2+} buffer, followed by the addition of diluted reaction mixture. Hereafter, the mixtures were placed under either 660 nm or 760 nm light condition to allow for the DrBphP-PSM to adopt its Pfr photo-state or Pr dark-dark state conformations, respectively. After 45 minutes incubation at room temperature with gentle rotation, the beads were washed twice with 200 μl of TBS-Mg^{2+} buffer. To recover the enriched ribosome-protein fusion, 200 μl of elution buffer (TBS buffer + 50 mM EDTA) was added to the beads and incubated at room temperature for 30 min with gentle rotation. The eluted solution was subjected to standard phenol–chloroform extraction and isopropanol

precipitation to remove protein components. Purified RNAs were subjected to reverse transcription using primers O8 with the SuperScript III (Thermo Fisher Scientific), and the enriched cDNA library was regenerated by PCR using primers O5 and O8 with KOD -Multi&Epi- DNA polymerase. After 6 rounds of the selections, the enriched DNA library was sequenced on an Illumina MiSeq machine using the Miseq Reagent Kit v.3 (150 cycles, 130 and 45 bp, paired-end).

Deep Sequencing Analysis

Only R1 reads of the paired-end reads were subjected to subsequent analysis. Analysis of the sequences was performed using custom python scripts (python 2.7). The sequences were filtered according to Phred quality scores (Q): reads were disregarded if more than half of the base calls were below Q20, and base calls with a quality score below Q20 were converted to N. For further quality assessment, sequences were searched for the two exact sequences at the constant region of an Affibody. It was assessed if the length between those two sites contained exactly 122 nucleotides. The sequences with expected length were considered to have a complete Affibody. Finally, we selected Affibody sequences that was enriched under 660 nm condition but not detectable under 760 nm condition.

Cell culture

HEK 293T and Neuro2a cells (ATCC) were cultured at 37 °C under 5% CO_2 in Dulbecco's modified Eagle's medium (DMEM; Sigma Aldrich) supplemented with 10% fetal bovine serum (FBS, HyClone, Utah, USA), 100 unit/ml penicillin and 100 μg/ml streptomycin (Gibco, California, USA). HeLa cells (ATCC) were cultured at 37 °C under 5% CO_2 in minimum essential media (Sigma Aldrich) supplemented with 10% FBS, 100 unit/ml penicillin and 100 μg/ml streptomycin. The cell lines were tested routinely for mycoplasma contamination to confirm there were no mycoplasma-contaminated cells in this study.

Light source

Except for split-fluc reassembly assay, light illumination was performed inside a CO_2 incubator. Preassembled LED arrays (CCS, Kyoto, Japan) with 660 nm and 760 nm wavelength were placed on the bottom of the incubator. For light illumination to cells, 24-well and 96-well plates were placed above the LED array. A regulated DC power supply (Kikusui Electronics Corporation, Kanagawa, Japan) was used for control of LED current flow. Temporal illumination pattern was generated by an Arduino mega microcontroller board. For split-fluc

reassembly assay, light illumination was performed using preassembled LED arrays with 660 nm and 800 nm wavelength in darkness outside of CO_2 incubator.

TetR-tetO-based gene expression system using luciferase reporter

HeLa cells were plated in the presence of 25 μM BV at 1.0×10^4 cells per well in a 96-well black-wall plate (Greiner, Frickenhausen, Germany) and cultured for 24 h at 37 °C in 5% CO_2. The cells were then transfected with Lipofectamine 3000 reagent (Invitrogen) according to the manufacturer's protocol. Plasmids encoding VP16-NLS, tetR and luciferase reporter were transfected at a 1:1:1 ratio. The total amount of DNA was 0.1 μg per well. As a mock-control Aff6-VP16-NLS (-) condition, the Aff6 moiety of Aff6-VP16-NLS was replaced with irrelevant Affibody; Zdk1[52]. Twenty-four hours after the transfection, the sample was added with 100 μl of fresh media, and then light illumination was applied at 37 °C in 5% CO_2. The red light samples were incubated under 660 nm pulsed light illumination (1 W m^{-2}) that is repeatedly switching on for 1 min and then turning off for 4 min. For the dark condition, HeLa cells were wrapped in aluminum foil and incubated at 37 °C in 5% CO_2. After incubation for 24 h, the culture medium was replaced with 100 μl of HBSS (Gibco) containing 500 μM $_D$-Luciferin (Wako Pure Chemical Industries) as a substrate. After 30 min at room temperature, bioluminescence measurements were performed with a Centro XS3 LB 960 plate-reading luminometer (Berthold Technologies, Bad Wildbad, Germany). When the SEAP reporter plasmid was used, supernatants of the illuminated cells were subjected to SEAP Reporter Gene Assay (Roche Diagnostics, Basel, Switzerland) according to the manufacturer's protocol.

Split-firefly luciferase (split-fluc) reassembly assay

HEK 293T cells were plated in the presence of 25 μM BV at 4.0×10^5 cells per well in 35-mm/ Tissue Culture Dish (Iwaki Glass, Chiba, Japan) and cultured for 24 h at 37 °C in 5% CO_2. Plasmids encoding Nfluc-DrBphP and 3xFLAG-Aff6_V18FΔN-Cfluc were transfected at a 1:1 ratio. The total amount of DNA was 2.5 μg per dish. In case of using plasmid encoding full-length fluc as a control, the amount of DNA was 0.025 μg per dish in order to align the dynamic range of bioluminescence intensity. Twenty-four hours after transfection, the culture medium was replaced with 2 ml of HBSS solution supplemented with 200 μM $_D$-Luciferin. After incubation for 30-min at room temperature, the sample was illuminated by 800 nm light (50 W m^{-2}) for 5-min using the 800 nm LED array to achieve photoconversion of DrBphP from the Pfr photo-state to Pr dark-state. Then, bioluminescence measurements were performed using a GloMax 20/20 Luminometer (Promega, Wisconsin, USA) at room temperature. The

bioluminescence signals were integrated over 1 s at room temperature and plotted every 1 s. To illuminate 660 nm light to the cells, we stopped the bioluminescence measurement and removed the sample dish from the luminometer. We then irradiated the sample dish with 660 nm light (10 W m^{-2}) for 1 min using the 660 nm LED array and immediately placed the sample dish back into the luminometer to resume the bioluminescence measurement. The procedures for illuminating 800 nm light to the cells were identical to those described above.

Luciferase reporter assay for CPTS design

HEK 293T and Neuro-2a cells were plated at 2.0×10^4 cells and HeLa cells were plated at 1.0×10^4 cells per well in a 96-well black-wall plate. The cells are cultured for 24 h at 37 °C in 5% CO_2. Plasmids encoding NLS-dCas9-NLS, MS2, p65-HSF1, sgRNA and luciferase reporter were transfected at a 1:1:1:1:1 ratio. The total amount of DNA was 0.1 μg per well. Procedures for light illumination of the MagRed system and bioluminescence detection were identical to those described above. For RpBphP1-PpsR2/QPAS1 systems, the red light samples were incubated under 760 nm pulsed light (1 min ON and 4 min OFF) of 10 W m^{-2}. The remaining procedures are identical to those described above. For the BV (+) condition, cells were plated in the presence of 25 μM BV and transfection were identical to those described above. Twenty-four hours after the transfection, the samples were added with 100 μl of fresh media supplemented with 25 μM BV. The remaining procedures are identical to those described above.

Endogenous gene activation by Red-CPTS

The procedures for plating and transfection were identical to those described above, except for using a mixture of sgRNAs separately targeting four endogenous genes and omitting the luciferase reporter. Forty-eight hours post-transfection, total RNA extraction and reverse transcription PCR were performed using CellAmp Direct RNA Prep Kit (Takara Bio) with PrimeScript Real-Time Master Mix (Takara Bio), according to the manufacturer's protocols. Quantitative PCR was performed by the StepOnePlus system (Thermo Fisher Scientific) using TaqMan Gene Expression Master Mix (Thermo Fisher Scientific). TaqMan primers and probes were used to quantify the expression level of target gene and GAPDH gene were measured as endogenous control (Life Technologies, TaqMan Gene Expression Assay IDs are as follows: ASCL1: Hs04187546_g1, IL1R2: Hs01030384_m1, HBG1: Hs00361131_g1, MYOD1: Hs02330075_g1, GAPDH: Hs99999905_m1). The ΔΔCt method was applied to show each relative mRNA level to negative controls transfected with empty vector.

Western blotting

HEK 293T cells were transiently transfected with plasmids encoding cysteine-eliminated mutants of DrBphP with either C24A or C24S, or RpBphP1 with either C20A or C20S. Twenty-four hours after the transfection, the cells were lysed in M-PER™ Mammalian Protein Extraction Reagent (Thermo Scientific). The cell extracts were adjusted to the same amount of total cellular protein (20 μg) and electrophoresed in a 10% polyacrylamide gel. After electrophoretic transfer to a nitrocellulose membrane, the membranes were blocked with TBS-T buffer (50 mM Tris-HCl, pH7.6, 150 mM NaCl, 0.05% Tween-20) containing 5% BSA (Sigma-Aldrich) for 1 h at room temperature. The antibody (V5 Tag Monoclonal Antibody conjugated with HRP, Invitrogen, Cat# R961-25, 1:1,000 dilution) in TBS-T containing 5% BSA were placed on the membrane and incubated for 1 h at room temperature. After three times washings with TBS-T over 5 min, detection was performed via ECL™ Prime Western Blotting System (GE Healthcare) and the blots were imaged with LAS-3000 system (Fujifilm Corporation, Tokyo, Japan).

Luciferase reporter assay for RedPA-Cre

HEK 293T cells were plated in the presence of 25 μM BV at 2.0×10^4 cells per well in a 96-well black-wall plate and cultured for 24 h at 37 °C in 5% CO_2. Plasmids encoding CreN, CreC fragments and luciferase reporter were transfected at a 1:1:8 ratio. The total amount of DNA was 0.1 μg per well. Six hours after the transfection, the sample was illuminated at 37 °C in 5% CO_2. For the MagRed system and nanoReD1/2 systems, the red light samples were incubated under 660 nm pulsed light (1 min ON and 4 min OFF) of 1 W m^{-2}. For RpBphP1-PpsR2/QPAS1, the red light samples were incubated under 760 nm pulsed light (1 min ON and 4 min OFF) of 10 W m^{-2}. For the dark condition, HEK 293T cell plates were wrapped in aluminum foil and incubated at 37 °C in 5% CO_2. After incubation for 18 hours, the culture medium was replaced with 100 μl of HBSS (Gibco) containing 200 μM D-Luciferin (Wako Pure Chemical Industries) as a substrate. After 30 min at room temperature, bioluminescence measurements were performed with the Centro XS3 LB 960 plate-reading luminometer.

Fluorescence reporter assay for RedPA-Cre

HEK 293T cells were plated at 0.8×10^5 cells per well in a 24-well plate and cultured for 24 h at 37 °C in 5% CO_2. Plasmids encoding NLS-CreN104-Aff6_V18FΔN-Venus, NLS-DrBphP (FL)-CreC106 and fluorescence reporter were transfected at a 1:1:8 ratio. The total amount of

DNA was 0.5 μg per well. Six hours after the transfection, the sample was illuminated at 37 °C in 5% CO_2. The red light samples were incubated under 660 nm pulsed light (1 min ON and 4 min OFF) of 1 W m^{-2}. For the dark condition, HEK 293T cell plates were wrapped in aluminum foil and incubated at 37 °C in 5% CO_2. After the incubation for 24 hours, cells were fixed with 4% paraformaldehyde in PBS (Wako Pure Chemical Industries) for 15 min, followed by blocking and permeabilization with incubation in blocking solution (5% BSA, 0.3% triton-X100 in PBS) for 1 h at room temperature. Then cells were immunostained with mouse anti-mCherry antibody (mCherry Monoclonal Antibody conjugated with Alexa Fluor 594, Invitrogen, Cat#M11240, 1:1,000 dilution) in blocking solution for 1 h at room temperature with gentle rocking. After three times washing with PBS, the cells were stained with 300 nM DAPI (Invitrogen) for 15 min at room temperature. After that, images were acquired using an inverted microscope (DMI6000B, Leica Microsystems, Wetzlar, Germany) equipped with a x10 objective (Leica HCX PL FLUOTAR 10x/0.30NA PH1) and an EM-CCD camera (Cascade II:512, Photometrics, Arizona, USA). The imaging of DAPI, GFP and mCherry channel was conducted with A, L5 and TX2 filter cube (Leica Microsystems)

Image processing

Obtained images were analyzed using FIJI version of imageJ[53] and CellProfiler[54]. The background of images was subtracted using build-in "Subtract background" tool in ImageJ. Nuclei were identified in the DAPI channel using an object diameter threshold of 5-20 pixel units. The mean intensity of Venus and mCherry fluorescence at each nucleus was measured in order to determine the population of GFP-positive (GFP^+) cells and mCherry positive (mCh^+) cells. The intensity threshold was determined not to detect mCh^+ cell in the mock-control condition. The number of mCh^+ cells was then divided by the number of GFP^+ cells and multiplied by 100 to obtain the percentage of mCh^+/GFP^+ cells.

***In vivo* RedPA-Cre activation**

All procedures involving animals were approved by the Institutional Animal Care and Use Committee of the University of Tokyo and were conducted in accordance with the Guidelines for Care and Use of Laboratory Animals as stated by the University of Tokyo. Livers of 4-week-old female ICR mice (Sankyo Labo Service Corporation, Inc., Tokyo, Japan) were hydrodynamically transfected by injecting 10 μg of bicistronic RedPA-Cre plasmid and 40 μg of bioluminescent reporter plasmid in TransIT-EE Hydrodynamic Delivery Solution (Mirus Bio LLC, Wisconsin, USA), according to the manufacturer's protocol. Eight hours after

injection, the abdominal surface fur of mice was removed using a depilatory cream and mice were randomly assigned to dark and red light group. The person performing the hydrodynamic injections was blinded as to the assignment. Mice of red light group were then illuminated with a LED light source (660 nm; 100 W m^{-2}, continuous). Every 8 hours, mice were temporally returned back to home-cage and fed for 1 h. Mice of dark group were kept in the home-cage that received no light. Bioluminescence imaging of the mice were performed 25 h after the hydrodynamic injection. Prior to bioluminescence imaging, 200 ml of 100 mM D-luciferin was intraperitoneally injected into the mice. Then, the mice were anaesthetized with isoflurane (Wako Pure Chemical Industries). Five minutes after the D-luciferin injection, bioluminescence images of the mice were obtained using the Lumazone bioluminescence imager (Nippon Roper, Chiba, Japan) equipped with the Evolve 512 EMCCD camera (Photometrics).

Statistics analysis

GraphPad Prism (version 9.0) was used for the statistical analyses: For comparison between two groups, a two-tailed unpaired Student's t-test was performed; For comparison between more than three groups, Ordinary two-way ANOVA was performed in; For determine the *P* value between of matched-pairs groups, the Wilcoxon matched-pairs signed rank test was performed. No sample size estimates were performed, and our sample sizes are consistent with those normally used in experiments for regulation of protein activity. No sample exclusion was carried out. A Life Sciences Reporting Summary for this paper is available.

Data and code availability

The read counts for all screening data are available on the DDBJ Sequence Read Archive, accession No. DRR243933 and DRR243934. The code for analysis of these data has been deposited on Github (https://github.com/Kazushi40/NGS_analysis). Source data for Figures 1,2,3,4 and 5 are available online. Other data and materials that support the findings of this study are available from the corresponding authors upon reasonable request.

Acknowledgements

This work was supported by CREST grant (JPMJCR1653) from the Japan Science and Technology Agency (to R.N., M.Y. and M.S.), and a project grant from Kanagawa Institute of Industrial Science and Technology (KISTEC) to M.S. Y. Kuwasaki was supported by KAKENHI-PROJECT-20J14492 for the JSPS Doctoral Course Students Research Fellow. K.S. was supported by Grant-in-Aid 18J01772 for the JSPS Research Fellow.

Author contributions

M.S. conceived the project and provided supervision. G.Y. developed the synthetic binder with support from Y.S. and performed preliminary tetR-tetO experiment. R.N. and K.F. measured absorption spectra of DrBphP and RpBphP1. Y. Kuwasaki and M.N. performed split-fluc reassembly assays. Y. Kakihara and Y. Kuwasaki performed experiments of tetR-tetO and Red-CPTS with help from T.N. M.N., K.S., R.B. and M.Y. performed experiments of RedPA-Cre. Y. Kuwasaki, K.S. and M.S wrote the manuscript and prepared the figures. R.B. and M.Y. edited the manuscript. All the authors checked and approved the manuscript.

Competing interests

The authors declare no competing interests.

References

1. Kennedy, M. J. *et al.* Rapid blue-light-mediated induction of protein interactions in living cells. *Nat. Methods* **7**, 973–975 (2010).

2. Guntas, G. *et al.* Engineering an improved light-induced dimer (iLID) for controlling the localization and activity of signaling proteins. *Proc. Natl. Acad. Sci. U. S. A.* **112**, 112–117 (2015).

3. Kawano, F., Suzuki, H., Furuya, A. & Sato, M. Engineered pairs of distinct photoswitches for optogenetic control of cellular proteins. *Nat. Commun.* **6**, 1–8 (2015).

4. Zhang, K. & Cui, B. Optogenetic control of intracellular signaling pathways. *Trends Biotechnol.* **33**, 92–100 (2015).

5. Losi, A., Gardner, K. H. & Möglich, A. Blue-Light Receptors for Optogenetics. *Chem. Rev.* **118**, 10659–10709 (2018).

6. Aoki, K. *et al.* Stochastic ERK activation induced by noise and cell-to-cell propagation regulates cell density-dependent proliferation. *Mol. Cell* **52**, 529–540 (2013).

7. Nihongaki, Y., Yamamoto, S., Kawano, F., Suzuki, H. & Sato, M. CRISPR-Cas9-based photoactivatable transcription system. *Chem. Biol.* **22**, 169–174 (2015).

8. Nihongaki, Y. *et al.* CRISPR-Cas9-based photoactivatable transcription systems to induce neuronal differentiation. *Nat. Methods* **14**, 963–966 (2017).

9. Nihongaki, Y., Kawano, F., Nakajima, T. & Sato, M. Photoactivatable CRISPR-Cas9 for optogenetic genome editing. *Nat. Biotechnol.* **33**, 755–760 (2015).

10. Nihongaki, Y., Otabe, T., Ueda, Y. & Sato, M. A split CRISPR–Cpf1 platform for inducible genome editing and gene activation. *Nat. Chem. Biol.* **15**, 882–888 (2019).

11. Kawano, F., Okazaki, R., Yazawa, M. & Sato, M. A photoactivatable Cre-loxP recombination system for optogenetic genome engineering. *Nat. Chem. Biol.* **12**, 1059–1064 (2016).

12. Jung, H. *et al.* Noninvasive optical activation of Flp recombinase for genetic manipulation in deep mouse brain regions. *Nat. Commun.* **10**, 314 (2019).

13. Lee, D. *et al.* Temporally precise labeling and control of neuromodulatory circuits in the mammalian brain. *Nat. Methods* **14**, 495–503 (2017).

14. Pu, J., Zinkus-Boltz, J. & Dickinson, B. C. Evolution of a split RNA polymerase as a versatile biosensor platform. *Nat. Chem. Biol.* **13**, 432–438 (2017).

15. Yu, D. *et al.* Optogenetic activation of intracellular antibodies for direct modulation of endogenous proteins. *Nat. Methods* **16**, 1095–1100 (2019).

16. Liu, Q. *et al.* A Photoactivatable Botulinum Neurotoxin for Inducible Control of Neurotransmission. *Neuron* **101**, 863-875.e6 (2019).

17. Ziegler, T. & Möglich, A. Photoreceptor engineering. *Front. Mol. Biosci.* **2**, 30 (2015).

18. Shimizu-Sato, S., Huq, E., Tepperman, J. M. & Quail, P. H. A light-switchable gene promoter system. *Nat. Biotechnol.* **20**, 1041–1044 (2002).

19. Levskaya, A., Weiner, O. D., Lim, W. A. & Voigt, C. A. Spatiotemporal control of cell signalling using a light-switchable protein interaction. *Nature* **461**, 997–1001 (2009).

20. Hochrein, L., Mitchell, L. A., Schulz, K., Messerschmidt, K. & Mueller-Roeber, B. L-SCRaMbLE as a tool for light-controlled Cre-mediated recombination in yeast. *Nat. Commun.* **9**, 1–10 (2018).

21. Kohchi, T., Kataoka, H. & Linley, P. J. Biosynthesis of chromophores for phytochrome and related photoreceptors. *Plant Biotechnol.* **22**, 409–413 (2005).

22. Wu, J. *et al.* A non-invasive far-red light-induced split-Cre recombinase system for controllable genome engineering in mice. *Nat. Commun.* **11**, (2020).

23. Yu, Y. *et al.* Engineering a far-red light-activated split-Cas9 system for remote-controlled genome editing of internal organs and tumors. *Sci. Adv.* **6**, (2020).

24. Kaberniuk, A., Shemetov, A. A. & Verkhusha, V. V. A bacterial phytochrome-based optogenetic system controllable with near-infrared light. *Nat. Methods* **13**, 591–597 (2016).

25. Redchuk, T. A., Omelina, E. S., Chernov, K. G. & Verkhusha, V. V. Near-infrared optogenetic pair for protein regulation and spectral multiplexing. *Nat. Chem. Biol.* **13**, 633–639 (2017).

26. Takala, H. *et al.* Signal amplification and transduction in phytochrome photosensors. *Nature* **509**, 245–248 (2014).

27. Wagner, J. R. *et al.* Mutational analysis of Deinococcus radiodurans bacteriophytochrome reveals key amino acids necessary for the photochromicity and proton exchange cycle of phytochromes. *J. Biol. Chem.* **283**, 12212–12226 (2008).

28. Takala, H., Lehtivuori, H., Hammarén, H., Hytönen, V. P. & Ihalainen, J. A. Connection between absorption properties and conformational changes in Deinococcus radiodurans phytochrome. *Biochemistry* **53**, 7076–7085 (2014).

29. Nord, K. *et al.* Binding proteins selected from combinatorial libraries of an α-helical bacterial receptor domain. *Nat. Biotechnol.* **15**, 772–777 (1997).

30. Paulmurugan, R. & Gambhir, S. S. Combinatorial library screening for developing an improved split-firefly luciferase fragment-assisted complementation system for studying protein-protein interactions. *Anal. Chem.* **79**, 2346–2353 (2007).

31. Taslimi, A. *et al.* Optimized second-generation CRY2-CIB dimerizers and photoactivatable Cre recombinase. *Nat. Chem. Biol.* **12**, 425–430 (2016).

32. Yao, S. *et al.* RecV recombinase system for in vivo targeted optogenomic modifications of single cells or cell populations. *Nat. Methods* **17**, 422–429 (2019).

33. Morikawa, K. *et al.* Photoactivatable Cre recombinase 3.0 for in vivo mouse applications. *Nat. Commun.* **11**, 2141 (2020).

34. Sternberg, N. & Hamilton, D. Bacteriophage P1 site-specific recombination. I. Recombination between loxP sites. *J. Mol. Biol.* **150**, 467–486 (1981).

35. Gierut, J. J., Jacks, T. E. & Haigis, K. M. Strategies to achieve conditional gene mutation in mice. *Cold Spring Harb. Protoc.* **2014**, 339–349 (2014).

36. Meinke, G., Bohm, A., Hauber, J., Pisabarro, M. T. & Buchholz, F. Cre Recombinase and Other Tyrosine Recombinases. *Chem. Rev.* **116**, 12785–12820 (2016).

37. Kim, H., Kim, M., Im, S.-K. & Fang, S. Mouse Cre-LoxP system: general principles to determine tissue-specific roles of target genes. *Lab. Anim. Res.* **34**, 147 (2018).

38. Huang, Z. *et al.* Creating Red Light-Controlled Protein Dimerization Systems as Genetically Encoded Actuators with High Specificity. *ACS Synth. Biol.* **9**, 3322–3333 (2020).

39. Boyden, E. S., Zhang, F., Bamberg, E., Nagel, G. & Deisseroth, K. Millisecond-timescale, genetically targeted optical control of neural activity. *Nat. Neurosci.* **8**, 1263–1268 (2005).

40. Dagliyan, O. *et al.* Computational design of chemogenetic and optogenetic split proteins. *Nat. Commun.* **9**, 4042 (2018).

41. Dolberg, T. B. *et al.* Computation-guided optimization of split protein systems. *Nat. Chem. Biol.* https://doi.org/10.1038/s41589-020-00729-8 (2021).

42. Legué, E. & Joyner, A. L. Genetic fate mapping using site-specific recombinases. *Methods Enzymol.* **477**, 153–181 (2010).

43. Pei, W. *et al.* Polylox barcoding reveals haematopoietic stem cell fates realized in vivo. *Nature* **548**, 456–460 (2017).

44. Fenno, L. E. *et al.* Targeting cells with single vectors using multiple-feature Boolean logic. *Nat. Methods* **11**, 763–772 (2014).

45. Weinberg, B. H. *et al.* Large-scale design of robust genetic circuits with multiple inputs and outputs for mammalian cells. *Nat. Biotechnol.* **35**, 453–462 (2017).

46. Takao, T. *et al.* Establishment of a tTA-dependent photoactivatable Cre recombinase knock-in mouse model for optogenetic genome engineering. *Biochem. Biophys. Res. Commun.* **526**, 213–217 (2020).

47. Nakamura, M., Gao, Y., Dominguez, A. A. & Qi, L. S. CRISPR technologies for precise epigenome editing. *Nat. Cell Biol.* **23**, 11–22 (2021).

48. Rees, H. A. & Liu, D. R. Base editing: precision chemistry on the genome and transcriptome of living cells. *Nat. Rev. Genet.* **19**, 770–788 (2018).

49. Müller, K. *et al.* A red/far-red light-responsive bi-stable toggle switch to control gene expression in mammalian cells. *Nucleic Acids Res.* **41**, e77 (2013).

50. Mukougawa, K., Kanamoto, H., Kobayashi, T., Yokota, A. & Kohchi, T. Metabolic engineering to produce phytochromes with phytochromobilin, phycocyanobilin, or phycoerythrobilin chromophore in Escherichia coli. *FEBS Lett.* **580**, 1333–1338 (2006).

51. Ohashi, H., Shimizu, Y., Ying, B. W. & Ueda, T. Efficient protein selection based on ribosome display system with purified components. *Biochem. Biophys. Res. Commun.* **352**, 270–276 (2007).

52. Wang, H. *et al.* LOVTRAP: An optogenetic system for photoinduced protein dissociation. *Nat. Methods* **13**, 755–758 (2016).

53. Schindelin, J. *et al.* Fiji: An open-source platform for biological-image analysis. *Nat. Methods* **9**, 676–682 (2012).

54. Carpenter, A. E. *et al.* CellProfiler: Image analysis software for identifying and quantifying cell phenotypes. *Genome Biol.* **7**, R100 (2006).

Figures

Figure 1: Development and characterization of MagRed.

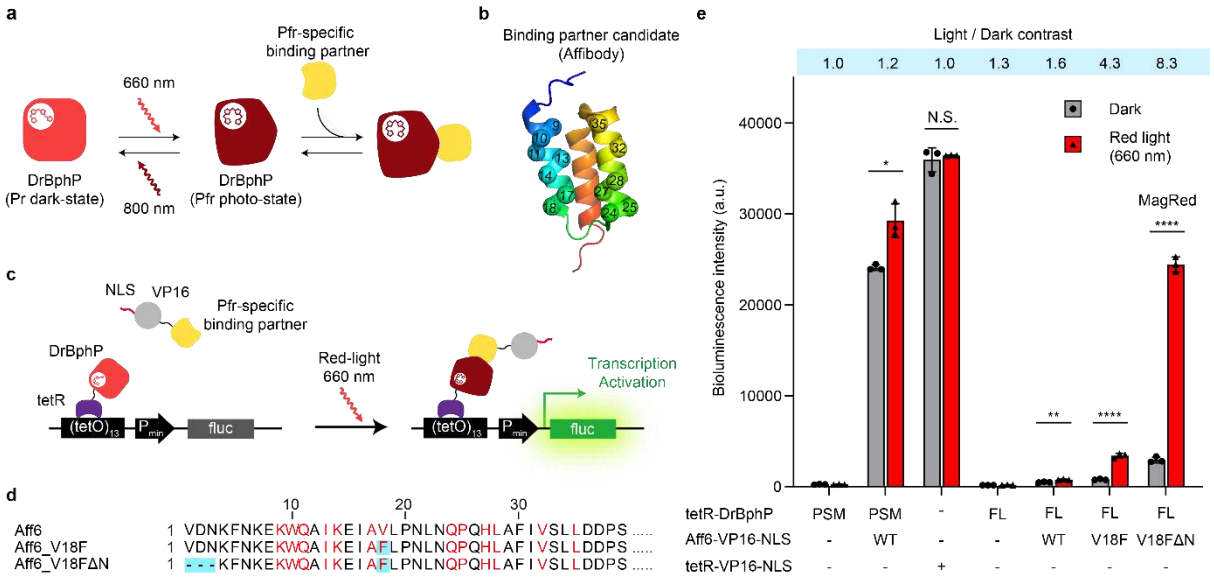

a, Schematic representation of DrBphP and its Pfr photo-state-specific binding partner. **b,** The diversified residues are rendered in ball-filling mode onto crystal structure of irrelevant Affibody (PDB: 2M5A). **c,** Schematic diagram of the tetR-tetO-based gene expression system using DrBphP and its Pfr photo-state-specific binding partner. Upon 660 nm light illumination, binding partner candidates fused with VP16 and NLS binds to the photoproduct of tetR-DrBphP anchored on the tetO element, thus activating transcription of the reporter fluc (NLS: nuclear localization signal, fluc: firefly luciferase, P_{min}: minimal cytomegalovirus promoter). **d,** Alignment of N-terminal amino acid sequence from Aff6 variants. The 13 residues diversified in the initial library are highlighted with red color and the residues altered from Aff6 are marked in cyan color. **e,** Bioluminescence intensity in HeLa cells transfected with different transcription activators and a bioluminescence reporter plasmid. (N.S. $P>0.05$; $*P<0.05$; $**P<0.01$; $****P<0.0001$; dark vs. light using two-tailed unpaired t-test, from three biologically independent samples, mean ± s.d.)

Figure 2: Split-firefly luciferase (split-fluc) reassembly assay for examining the association and dissociation of MagRed.

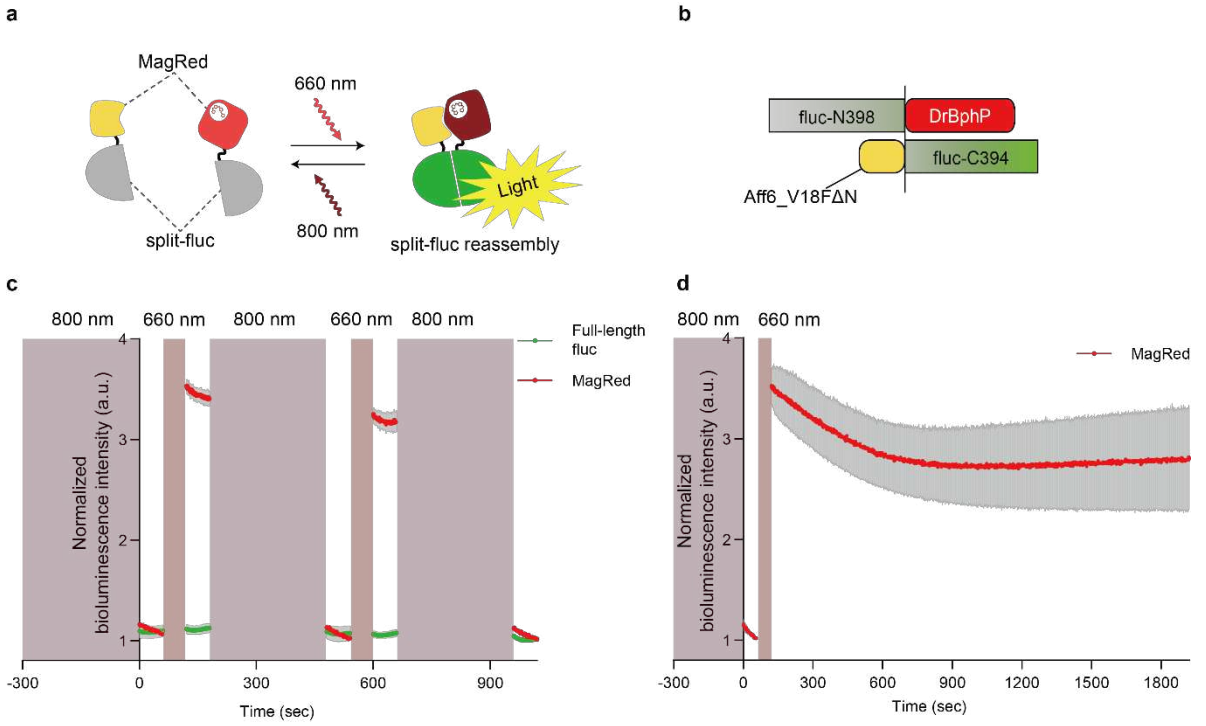

a, Schematic representation of split-fluc reassembly assay. Upon 660 nm light illumination, MagRed-fused split-fluc halves are assembled, leading to a bioluminescence signal increase. Upon 800 nm illumination, MagRed-fused split-fluc halves are dissociated, leading to a bioluminescence signal decrease. **b,** Schematics of domain structures of the fusion proteins. Newly created N- and C-termini of split-fluc halves (fluc-N398: residues 1–398 and fluc-C394: residues 394–550) were fused with DrBphP and Aff6_V18FΔN, respectively. **c,** Representative time-course of bioluminescence changes of MagRed-fused split-fluc halves and full-length fluc upon repeated illumination at 660 nm (10 W m^{-2}) for one-minute and 800 nm (50 W m^{-2}) for five-minutes. Bioluminescence signals were normalized to the minimum intensity within each sample. (n = 3 biologically independent samples, mean ± s.d.) **d,** Representative time-course of bioluminescence intensity for 30 min after turning off the 660 nm illumination (10 W m^{-2}). Bioluminescence signals were normalized to the minimum intensity within each sample. (n = 3 biologically independent samples, mean ± s.d.)

Figure 3: Comparison of MagRed and RpBphP1-PpsR2/QPAS1 in CPTS system.

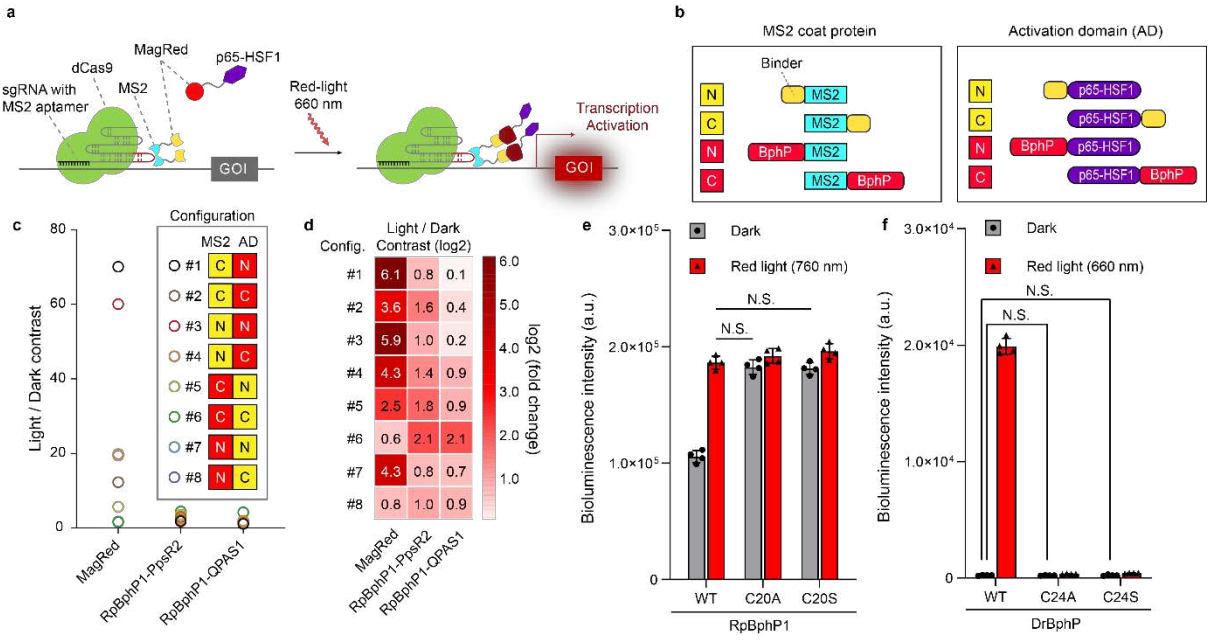

a, Schematic of the Red-CPTS system. Catalytically inactive Cas9 (dCas9) and sgRNA bearing MS2 RNA aptamers works as a genomic anchor. MagRed was fused to the transcription activation domain p65-HSF1 and MS2 coat protein. Upon 660 nm light illumination, p65-HSF1 was recruited to target loci by MagRed interaction, activating transcription of targeted genes. **b, c, d**, Comprehensive CPTS architectures with fusing BphP or its binder to either the N- or C- terminus of the p65-HSF1 transactivation domain and MS2 coat protein. The tested combination of MS2 and p65-HSF1 was displayed in **b**. Mean Light/Dark contrasts of all tested combinations are plotted with real number scale in **c**, and are shown as a heatmap with log2 scale in **d**. These Light/Dark contrasts were calculated based on bioluminescence intensity of HEK 293T cells transfected with different CPTS designs and a bioluminescence reporter plasmid. See Supplementary Figure. 7 for detailed results of each combination (mean from n=3 biological replicates). **e**, **f** Cysteine mutagenesis of RpBphP1 (**e**) and DrBphP to examine the contribution of their apo-proteins in CPTS. Experimental conditions were the same as those in **c** and **d**. Control constructs with mutations at either C20A or C20S of RpBphP1 exhibited high bioluminescence intensity comparable to that of RpBphP1 WT at red light condition in **e**, whereas those at either C24A or C24S of DrBphP abolished the bioluminescence in **f**. Bar data are shown as mean ± s.d. from four biological replicates (N.S. $P > 0.05$; two-way ANOVA with multiple comparison).

Figure 4: MagRed-mediated optogenetic control of endogenous transcription in mammalian cells.

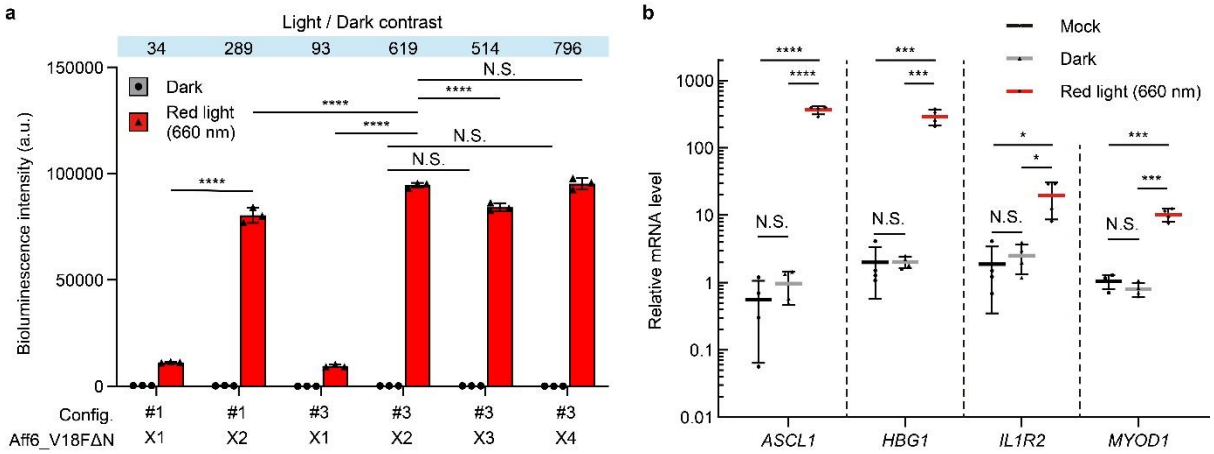

a, Bioluminescence intensity in HEK 293T cells transfected with different Red-CPTS designs and a bioluminescence reporter plasmid. (****P < 0.0001; two-way ANOVA with multiple comparison, n = 3 biologically independent samples, mean ± s.d.). **b,** Simultaneous activation of multiple endogenous gene targets was achieved using a mixture of gRNAs targeted to *ASCL1*, *HBG1*, *IL1R2* and *MYOD1* in HEK 293T cells. (N.S. P>0.05; *P < 0.1; ***P < 0.001; ****P < 0.0001; two-way ANOVA with multiple comparison, n = 4 biologically independent samples, mean ± s.d.)

Figure 5: A photoactivatable Cre-*loxP* recombination system based on the MagRed system.

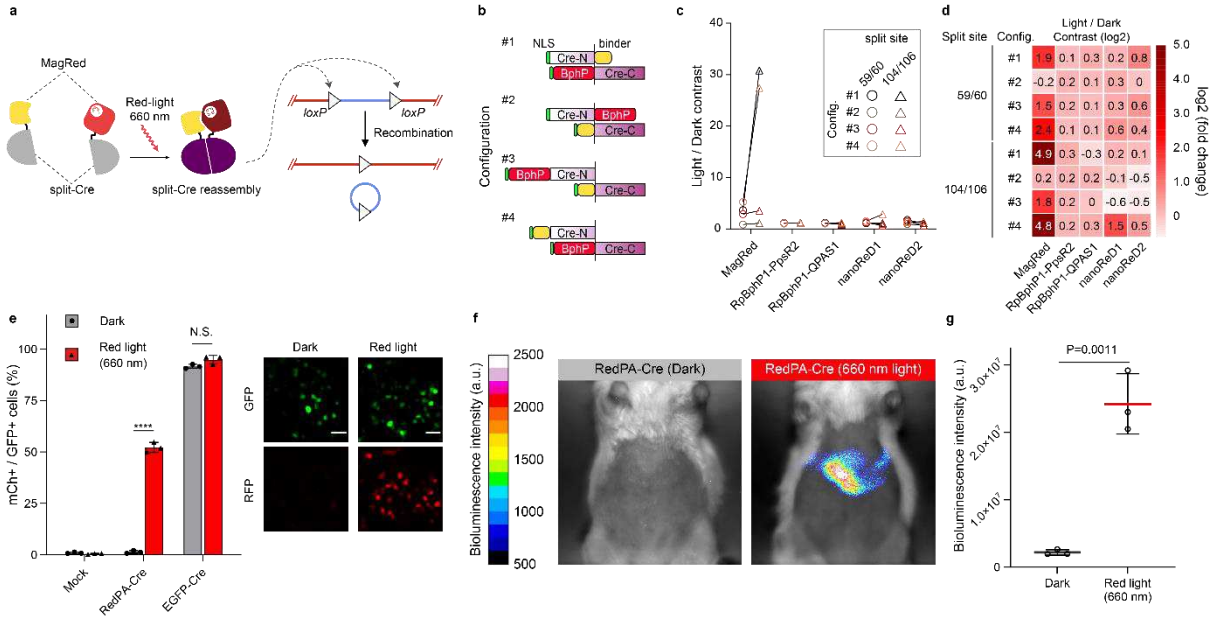

a, Schematic representation of RedPA-Cre. Upon 660 nm light illumination, split-Cre fragments reassembly is induced by the light-inducible association of MagRed, leading to recombination of DNA sequences flanked by two *loxP* sites. **b,** Comprehensive RedPA-Cre designs with combination of four configurations and the two split positions of Cre. **c, d,** Mean Light/Dark contrasts of all tested combinations are plotted with real number scale in **c**, and are shown as a heatmap with log2 scale in **d**. These Light/Dark contrasts were calculated based on bioluminescence intensity of HEK 293T cells transfected with different RedPA-Cre designs and a bioluminescence reporter plasmid. See Supplementary Figure. 12 for detailed results of each combination (mean from n=4 biological replicates). **e,** Fluorescence reporter (mCherry) assay with RedPA-Cre tagged with yellow fluorescent protein Venus. The percentage of mCherry positive cells among GFP positive cells (mCh^+/GFP^+) was estimated from >1000 cells of three independent experiments. (N.S. $P>0.05$; ****$P < 0.0001$; dark vs. light using two-tailed unpaired t-test, mean ± s.d.). Scale bars, 20 μm. **f,** Comparison of bioluminescence images of mice maintained in the dark and subjected to the illumination. The fluc expression was measured using 200 μl of 100 mM D-luciferin 25 h after transfection. **g,** Comparison of bioluminescence intensities of mice maintained in the dark and subjected to the illumination. Gray and Red bars represent the mean ± s.d. bioluminescence intensity and black dots represent the bioluminescence intensity of each mouse (n = 3 mice per group). (Dark vs. 660 nm light using two-tailed unpaired t-test)

Figures

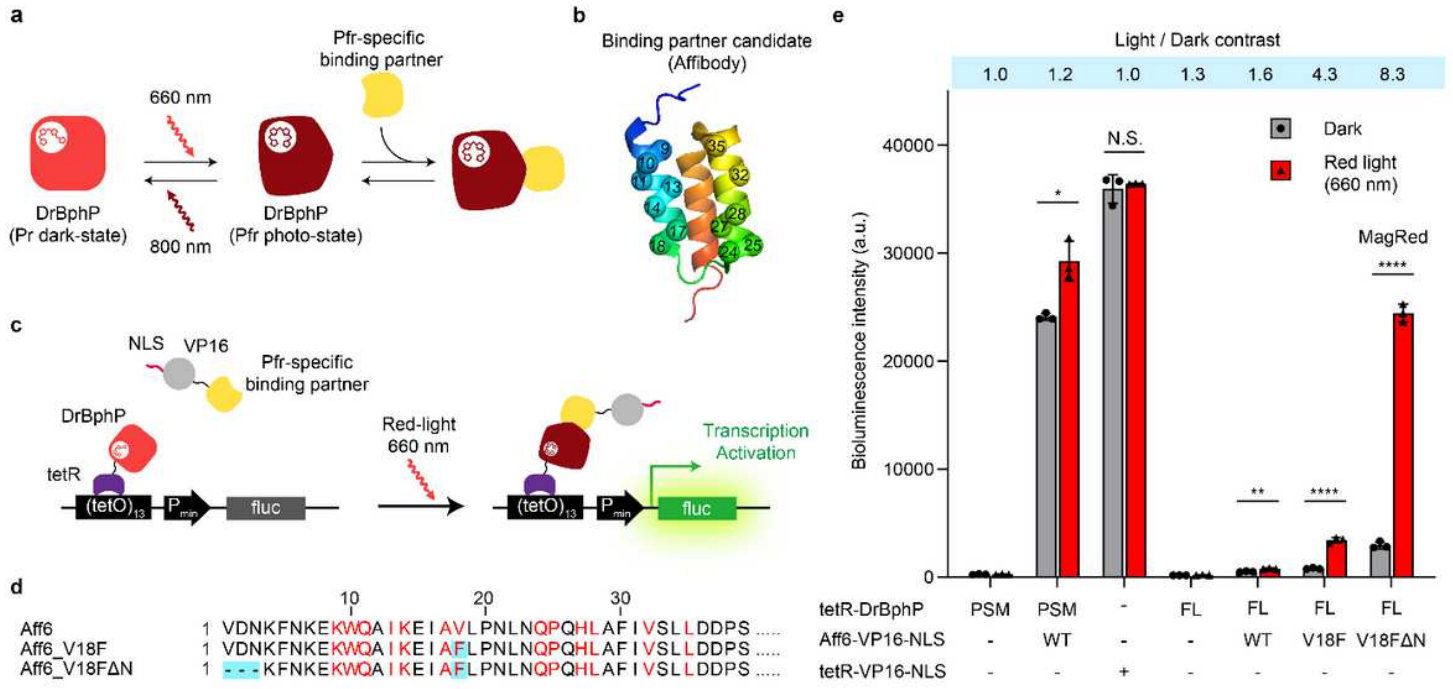

Figure 1

Development and characterization of MagRed. a, Schematic representation of DrBphP and its Pfr photo-state-specific binding partner. b, The diversified residues are rendered in ball-filling mode onto crystal structure of irrelevant Affibody (PDB: 2M5A). c, Schematic diagram of the tetR-tetO-based gene expression system using DrBphP and its Pfr photo-state-specific binding partner. Upon 660 nm light illumination, binding partner candidates fused with VP16 and NLS binds to the photoproduct of tetR-DrBphP anchored on the tetO element, thus activating transcription of the reporter fluc (NLS: nuclear localization signal, fluc: firefly luciferase, Pmin: minimal cytomegalovirus promoter). d, Alignment of N-terminal amino acid sequence from Aff6 variants. The 13 residues diversified in the initial library are highlighted with red color and the residues altered from Aff6 are marked in cyan color. e, Bioluminescence intensity in HeLa cells transfected with different transcription activators and a bioluminescence reporter plasmid. (N.S. $P>0.05$; *$P < 0.05$; **$P < 0.01$; ****$P < 0.0001$; dark vs. light using two-tailed unpaired t-test, from three biologically independent samples, mean ± s.d.)

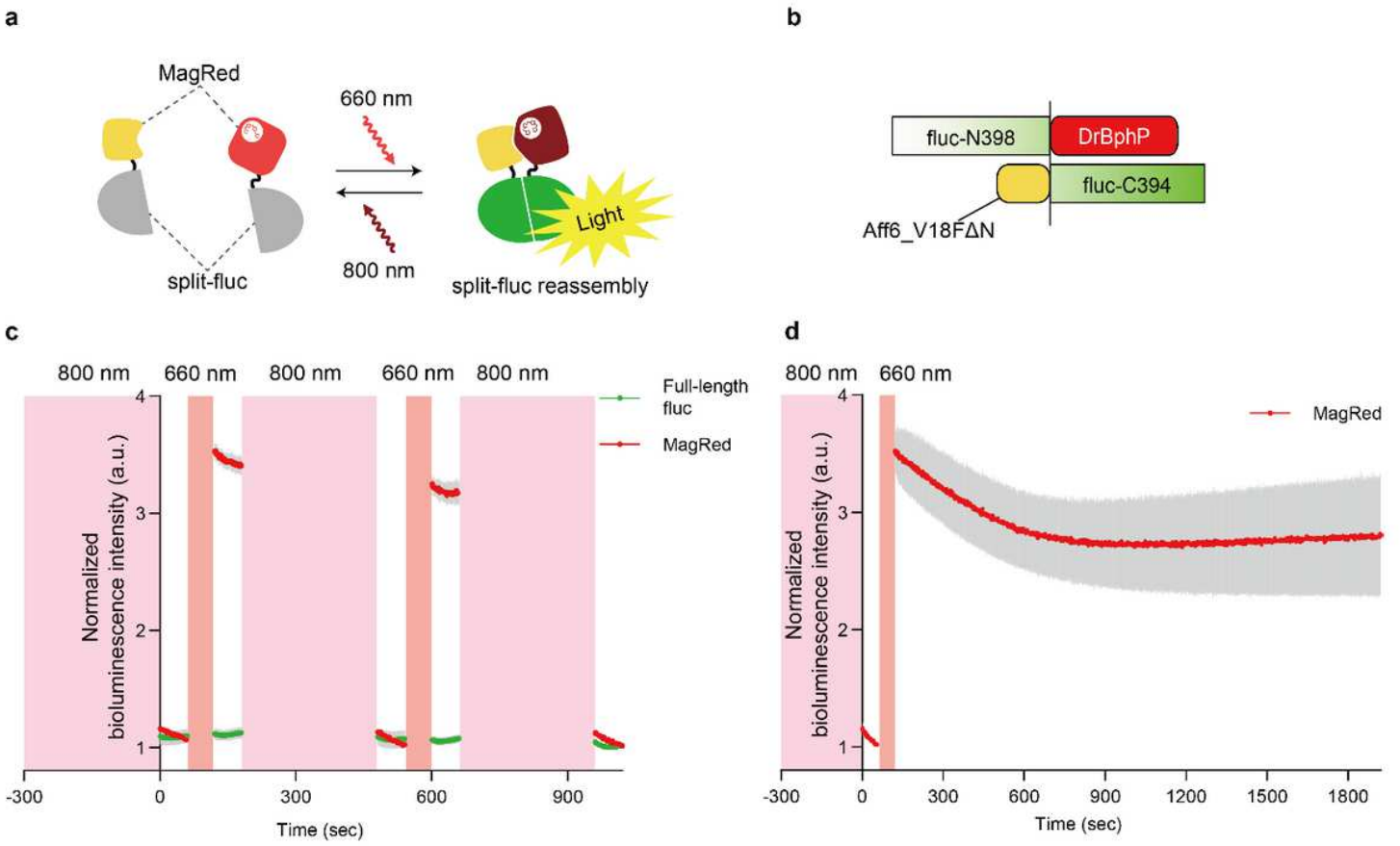

Figure 2

Split-firefly luciferase (split-fluc) reassembly assay for examining the association and dissociation of MagRed. a, Schematic representation of split-fluc reassembly assay. Upon 660 nm light illumination, MagRed-fused split-fluc halves are assembled, leading to a bioluminescence signal increase. Upon 800 nm illumination, MagRed-fused split-fluc halves are dissociated, leading to a bioluminescence signal decrease. b, Schematics of domain structures of the fusion proteins. Newly created N- and C-termini of split-fluc halves (fluc-N398: residues 1–398 and fluc-C394: residues 394–550) were fused with DrBphP and Aff6_V18FΔN, respectively. c, Representative time-course of bioluminescence changes of MagRed-fused split-fluc halves and full-length fluc upon repeated illumination at 660 nm (10 W m-2) for one-minute and 800 nm (50 W m-2) for five-minutes. Bioluminescence signals were normalized to the minimum intensity within each sample. (n = 3 biologically independent samples, mean ± s.d.) d, Representative time-course of bioluminescence intensity for 30 min after turning off the 660 nm illumination (10 W m-2). Bioluminescence signals were normalized to the minimum intensity within each sample. (n = 3 biologically independent samples, mean ± s.d.)

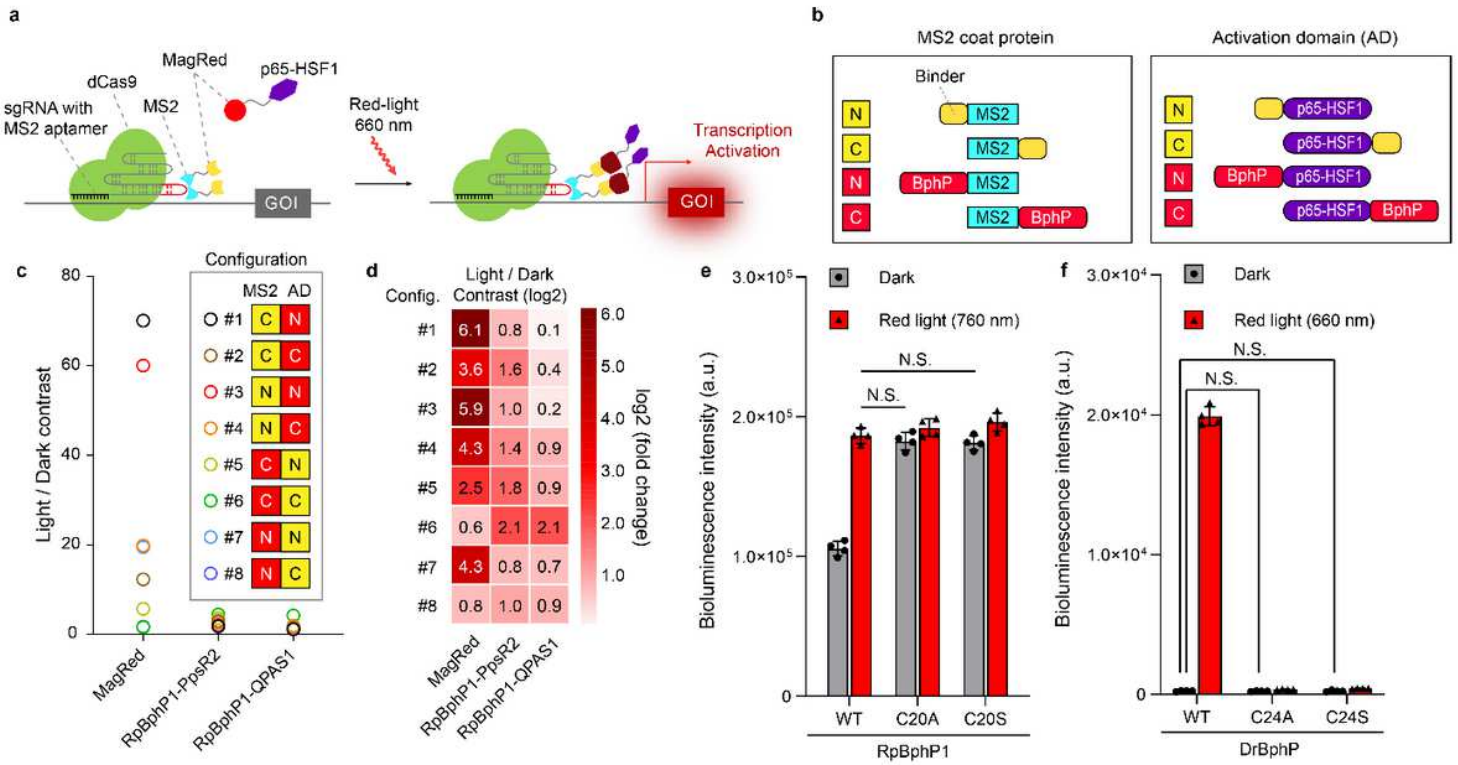

Figure 3

Comparison of MagRed and RpBphP1-PpsR2/QPAS1 in CPTS system. a, Schematic of the Red-CPTS system. Catalytically inactive Cas9 (dCas9) and sgRNA bearing MS2 RNA aptamers works as a genomic anchor. MagRed was fused to the transcription activation domain p65-HSF1 and MS2 coat protein. Upon 660 nm light illumination, p65-HSF1 was recruited to target loci by MagRed interaction, activating transcription of targeted genes. b, c, d, Comprehensive CPTS architectures with fusing BphP or its binder to either the N- or C- terminus of the p65-HSF1 transactivation domain and MS2 coat protein. The tested combination of MS2 and p65-HSF1 was displayed in b. Mean Light/Dark contrasts of all tested combinations are plotted with real number scale in c, and are shown as a heatmap with log2 scale in d. These Light/Dark contrasts were calculated based on bioluminescence intensity of HEK 293T cells transfected with different CPTS designs and a bioluminescence reporter plasmid. See Supplementary Figure. 7 for detailed results of each combination (mean from n=3 biological replicates). e, f Cysteine mutagenesis of RpBphP1 (e) and DrBphP to examine the contribution of their apo-proteins in CPTS. Experimental conditions were the same as those in c and d. Control constructs with mutations at either C20A or C20S of RpBphP1 exhibited high bioluminescence intensity comparable to that of RpBphP1 WT at red light condition in e, whereas those at either C24A or C24S of DrBphP abolished the bioluminescence in f. Bar data are shown as mean ± s.d. from four biological replicates (N.S. $P > 0.05$; two-way ANOVA with multiple comparison).

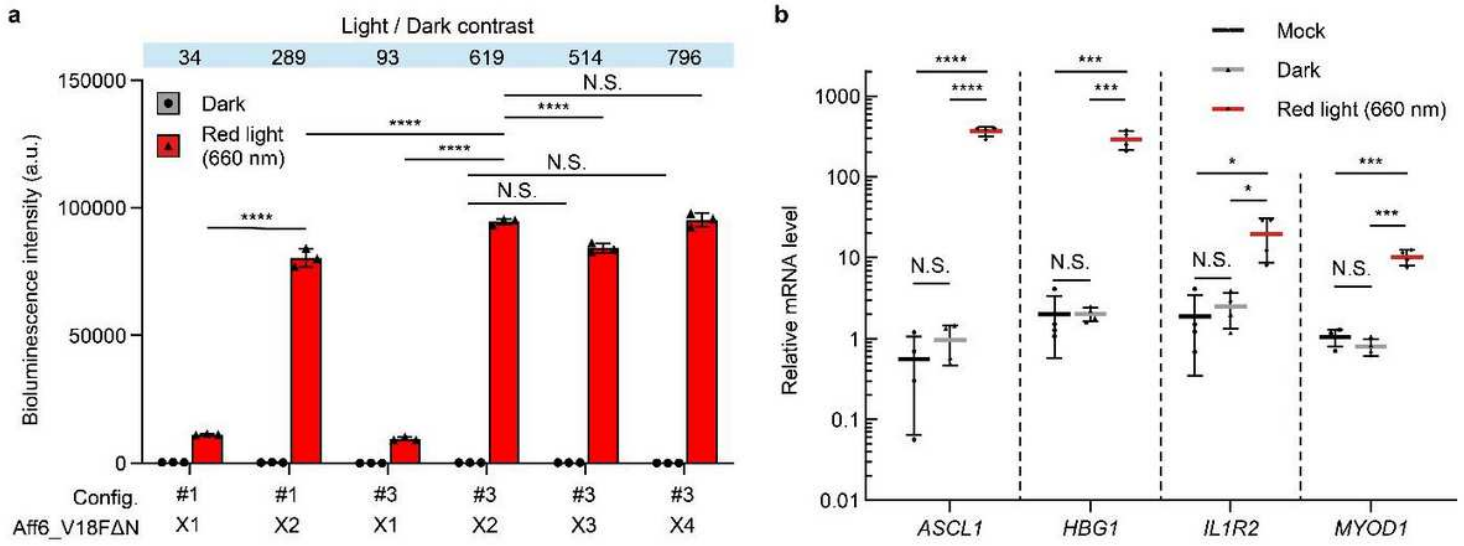

Figure 4

MagRed-mediated optogenetic control of endogenous transcription in mammalian cells. a, Bioluminescence intensity in HEK 293T cells transfected with different Red-CPTS designs and a bioluminescence reporter plasmid. (****P < 0.0001; two-way ANOVA with multiple comparison, n = 3 biologically independent samples, mean ± s.d.). b, Simultaneous activation of multiple endogenous gene targets was achieved using a mixture of gRNAs targeted to ASCL1, HBG1, IL1R2 and MYOD1 in HEK 293T cells. (N.S. P>0.05; *P < 0.1; ***P < 0.001; ****P < 0.0001; two-way ANOVA with multiple comparison, n = 4 biologically independent samples, mean ± s.d.)

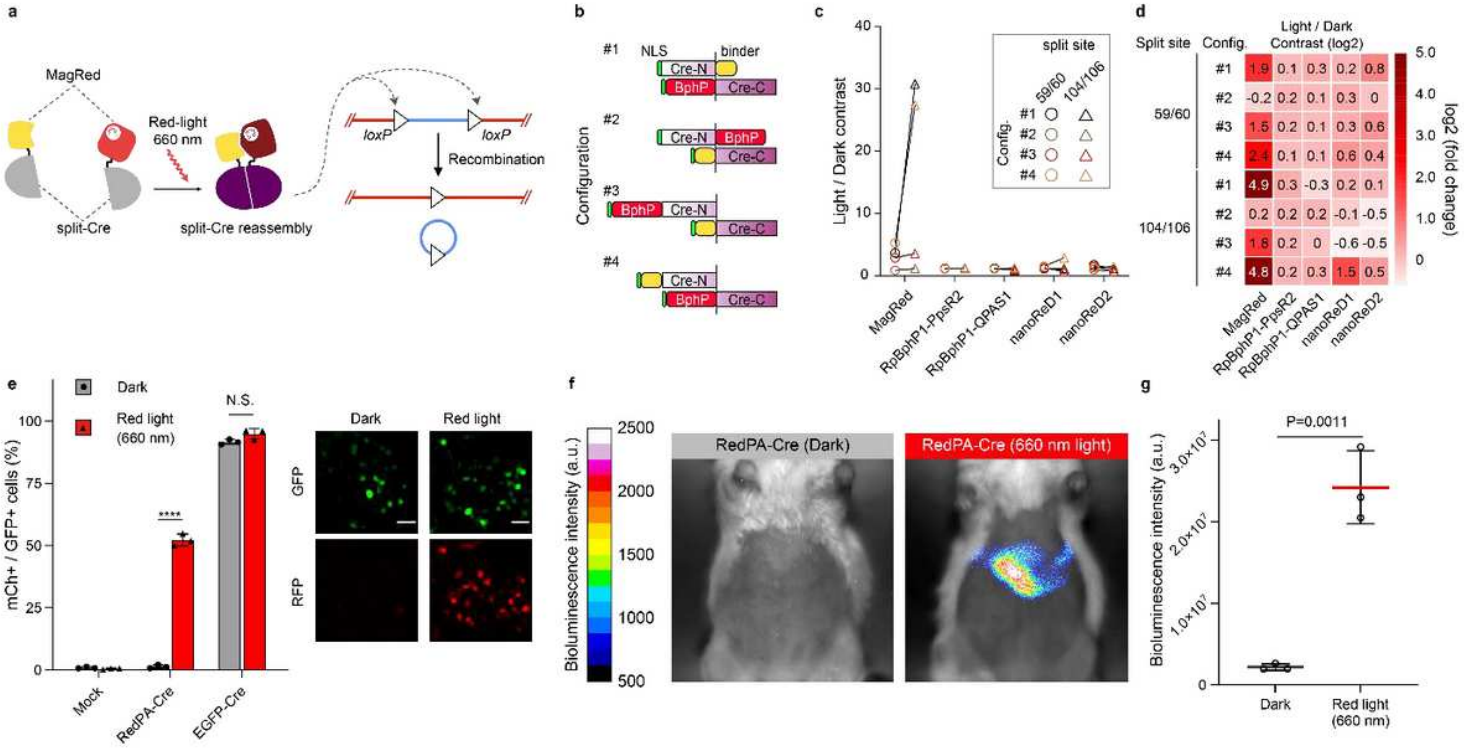

Figure 5

A photoactivatable Cre-loxP recombination system based on the MagRed system. a, Schematic representation of RedPA-Cre. Upon 660 nm light illumination, split-Cre fragments reassembly is induced by the light-inducible association of MagRed, leading to recombination of DNA sequences flanked by two loxP sites. b, Comprehensive RedPA-Cre designs with combination of four configurations and the two split positions of Cre. c, d, Mean Light/Dark contrasts of all tested combinations are plotted with real number scale in c, and are shown as a heatmap with log2 scale in d. These Light/Dark contrasts were calculated based on bioluminescence intensity of HEK 293T cells transfected with different RedPA-Cre designs and a bioluminescence reporter plasmid. See Supplementary Figure. 12 for detailed results of each combination (mean from n=4 biological replicates). e, Fluorescence reporter (mCherry) assay with RedPA-Cre tagged with yellow fluorescent protein Venus. The percentage of mCherry positive cells among GFP positive cells (mCh+/GFP+) was estimated from >1000 cells of three independent experiments. (N.S. $P>0.05$; ****$P < 0.0001$; dark vs. light using two-tailed unpaired t-test, mean ± s.d.). Scale bars, 20 μm. f, Comparison of bioluminescence images of mice maintained in the dark and subjected to the illumination. The fluc expression was measured using 200 μl of 100 mM D-luciferin 25 h after transfection. g, Comparison of bioluminescence intensities of mice maintained in the dark and subjected to the illumination. Gray and Red bars represent the mean ± s.d. bioluminescence intensity and black dots represent the bioluminescence intensity of each mouse (n = 3 mice per group). (Dark vs. 660 nm light using two-tailed unpaired t-test)

Supplementary Files

This is a list of supplementary files associated with this preprint. Click to download.

- SupplementaryNoteKuwasaki.pdf
- SupplementaryinformationKuwasaki.pdf